Photocatalysis

DOI: 10.1002/anie.201007869

Titanium(IV) Dioxide Surface-Modified with Iron Oxide as a Visible Light Photocatalyst **

Hiroaki Tada, Qiliang Jin, Hiroaki Nishijima, Hironori Yamamoto, Musashi Fujishima, Shin-ichi Okuoka, Takanori Hattori, Yasutaka Sumida, and Hisayoshi Kobayashi*

TiO_2 has three polymorphic forms: anatase, rutile, and brookite. Anatase usually has the highest photocatalytic activity under illumination of UV light; the activity can further be improved by coupling with rutile.[1] The development of a general method for endowing commercial anatase and anatase–rutile composite TiO_2 with visible-light response and concomitantly increasing their UV-light activity should dramatically expand their viability. To this end, doping of various transition metals and anions has been extensively studied.[2–8] In particular iron, which is harmless and abundant in nature is an ideal candidate; however, the positive doping effect is only limited to TiO_2 particles smaller than 10 nm in diameter.[9–12] This limit mainly arises because the doping generates impurity and/or vacancy levels in the bulk, which act as the recombination centers. As an alternative, Kisch et al. have devised the photosensitization of TiO_2 by surface modification with platinum(IV) chloride.[13] This approach is attractive in that the visible-light response can be induced by the simple procedure without introduction of the impurity/vacancy levels. Recently, the research groups of Ohno[14] and Hashimoto[15] have shown that the surface modification of rutile TiO_2 with Fe^{3+} by the impregnation method leads to high visible-light activities for the decomposition of model organic pollutants. However, the effect is small for anatase TiO_2. On the other hand, we have developed the chemisorption–calcination cycle (CCC) technique, in which metal complexes are adsorbed by chemical bonds and the organic (ligand) part is oxidized by post-heating to prepare metal oxide clusters and ultrathin films at a molecular scale.[16]

Herein we show that the surface modification of two kinds of TiO_2 particles (see the Experimental Section) with highly dispersed iron oxides by the CCC technique ($(FeO_x)_m/TiO_2$) gives rise to a high level of visible-light-induced activity and greatly heightens the activity under UV-light irradiation. $[Fe(acac)_3]$ was adsorbed on the TiO_2 surface by a partial ligand exchange between the acetylacetonate and surface OH groups [Equation (1)]

$$[Fe(acac)_3] + l\,(Ti_s{-}OH) \rightarrow [Fe(acac)_{3-l}(O{-}Ti_s)_l] + l\,AcacH \qquad (1)$$

where the subscript s denotes the surface atom and $l \approx 1$.

By the CCC technique utilizing this reaction, $(FeO_x)_m/TiO_2$ was prepared (see the Experimental Section). This technique is designed to form not FeO_x clusters but the isolated iron oxide species on TiO_2 by using $[Fe(acac)_3]$ as a precursor and a non-aqueous solvent to restrict hydrolysis polymerization. In the procedures, the elimination of the physisorbed complexes before calcination is crucial for the photocatalytic activity, although a similar impregnation method using $[Fe(acac)_3]$ without the rinsing process was reported.[17,18] For comparison, Pt/WO_3 with a high visible-light-induced activity[19] was also prepared. FTIR spectra confirmed that the signals that are due to the residual acetylacetonate ligands of the chemisorbed species disappear after the heating. The Fe on the TiO_2 surface was dissolved by the treatment with 35% HCl, and the $(FeO_x)_m$/P-25 solid was completely dissolved into 96% H_2SO_4 at 353 K. The amount of Fe in the former solution was in agreement with that in the latter solution, which indicates the existence of the Fe only on the surface. The Fe loading amount is expressed by the number of Fe^{3+} ions per unit TiO_2 surface area (Γ/ions nm^{-2}).

The adsorption isotherm of $[Fe(acac)_3]$ on P-25 at 298 K shows that the adsorption amount steeply increases with increasing equilibrium concentration to reach a saturated value at more than 4×10^{-3} mol dm^{-3} (Supporting Information, Figure S1). Good linearity of the Langmuir plot is consistent with the fact that $[Fe(acac)_3]$ is chemisorbed on the TiO_2 surface. The saturated adsorption amount was determined to be 0.46 ions nm^{-2}. In common with the impregnation samples ($(FeO_x)_n/TiO_2$), a weak electronic absorption around 470 nm (B_1) is present along with the absorption at 410 nm (B_2).[14,15,17,18] The absorption bands of B_1 and B_2 were attributed to the d–d transition and to the electronic transition from Fe^{3+} levels to the conduction band (cb) of TiO_2, respectively.[12] Upon chemically doping Cr and N ions into TiO_2, similar weak shoulders appear in the visible region owing to the formation of localized impurity levels within the band gap.[8] In contrast, the absorption spectra of $(FeO_x)_m/TiO_2$ (Figure 1) appear to show a marked band gap narrowing from 3.3 to 2.85 eV as Γ increases. This spectral feature was

[*] Prof. Dr. H. Tada, Q. Jin, H. Nishijima, H. Yamamoto, Dr. M. Fujishima
Department of Applied Chemistry
School of Science and Engineering, Kinki University 3-4-1 Kowakae, Higashi-Osaka, Osaka 577-8502 (Japan)
S.-i. Okuoka, T. Hattori, Y. Sumida
Advanced Materials Research Center, Nippon Shokubai Co. Ltd. 5-8, Nishi Otabi-cho, Suita, Osaka 564-8512 (Japan)
Prof. Dr. H. Kobayashi
Department of Chemistry and Materials Technology, Kyoto Institute of Technology, Matsugasaki, Sakyo-ku, Kyoto, 606-8585 (Japan)

[**] XAFS measurements were performed at the Spring-8 with approval of the Japan Synchrotron Radiation Research Institute (JASRI). This work was supported by a Grant-in-Aid for Scientific Research (B) No. 20350097 from the Ministry of Education, Science, Sport, and Culture (Japan).

Supporting information for this article is available on the WWW under http://dx.doi.org/10.1002/anie.201007869.

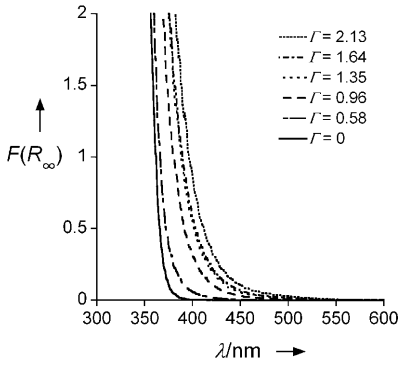

Figure 1. UV/Vis absorption spectra of $(FeO_x)_m$/mp-TiO_2/FTO prepared by the CCC technique.

also observed for TiO_2 doped with Cr[6] and N[7] using the physical methods of ion implantation and magnetron sputtering. High-resolution transmission electron microscopic observation of $(FeO_x)_m/TiO_2$ confirmed no particles on the TiO_2 surface at $\Gamma < 1$ ions nm^{-2}.

To obtain structural information, Fe K-edge X-ray absorption fine structure spectra were measured. Figure 2a shows X-ray absorption near-edge structure (XANES) spectra for iron metal and several iron oxides. The absorption edge of $(FeO_x)_m/TiO_2$ is in agreement with that of α-Fe_2O_3, which indicates that the iron oxidation state is +3 under such high-energy X-ray irradiation. Figure 2b shows the Fourier transforms of the k^3-weighted X-ray absorption fine structure (EXAFS) for $(FeO_x)_m/TiO_2$. The peaks around 1.55 Å seen for all of the samples arise from the Fe–O scattering. The peak top position of $(FeO_x)_m/TiO_2$ increases from 1.50 Å at $\Gamma = 5.39$ to 1.60 Å at $\Gamma = 0.22$, while $(FeO_x)_n/TiO_2$ has a constant Fe–O distance of 1.53 Å (Supporting Information, Figure S2a). The change in the peak top position would reflect the Fe–O distance perturbed by the Ti_s–O–Fe interfacial bond, which is predicted to become pronounced as the cluster size decreases. The pre-edge in the XANES spectra resulting from the forbidden 1s→3d transition affords information on the coordination symmetry around the iron ion.[20] The normalized peak height of the pre-edge for $(FeO_x)_m/TiO_2$ is smaller than those for γ-Fe_2O_3 and α-Fe_2O_3, depending on Γ with a minimum at $\Gamma = 0.5$ (Supporting Information, Figure S2b). The iron ion in $(FeO_x)_m/TiO_2$ is suggested to have a higher coordination symmetry compared to those in the bulk crystals. These results indicate that unique iron oxides are formed on the TiO_2 surface in an extremely highly dispersed state ($m < n$) without diffusion into the bulk.

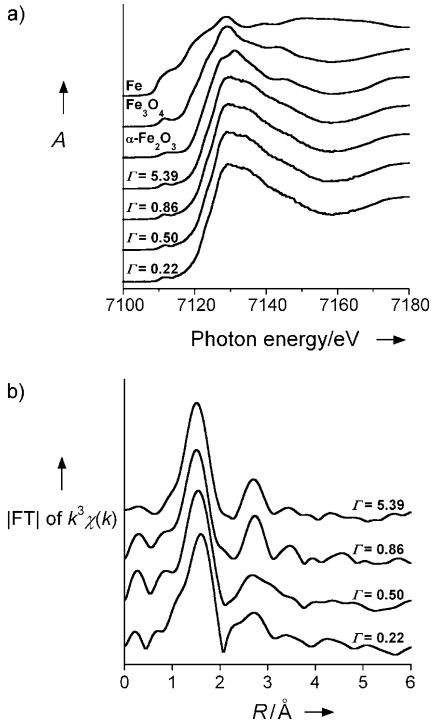

Figure 2. XANES and EXAFS spectra. a) XANES spectra for Fe, Fe_3O_4, α-Fe_2O_3, and $(FeO_x)_m/TiO_2$ at various Γ. b) Fourier transforms of the k^3-weighted EXAFS spectra for $(FeO_x)_m/TiO_2$.

To assess the relative photocatalytic activities of $(FeO_x)_m/TiO_2$ with respect to those of P-25 and ST-01, which are widely used as standard photocatalysts, the pseudo rate constants were determined under the same irradiation conditions with the same amount of photocatalysts. As a liquid-phase test reaction, the photocatalytic degradation of 2-naphthol (2-NAP) was carried out under illumination with visible light ($\lambda > 400$ nm, $I_{420-485\,nm} = 1.0$ mW cm^{-2}) and UV light ($330 < \lambda < 400$ nm, $I_{320-400\,nm} = 0.5$ mW cm^{-2}). 2-NAP is the starting material of azo dyes and is used as a model water pollutant.[22] 2-NAP has an absorption band centered at 224 nm owing to the $n \rightarrow \pi^*$ transition. On irradiation with visible light (Figure 3a) or UV light (Figure 3b) in the presence of $(FeO_x)_m$/P-25, the decomposition of 2-NAP proceeds, whereas it hardly occurs without photocatalysts. Figure 3c shows the first-order pseudo rate constants for illumination with visible light (k_{vis}) and UV light (k_{UV}) as a function of Γ. The surface modification of P-25 develops a high level of visible-light-induced activity, $k_{vis} = (0.69 \pm 0.02)$ h^{-1} at $\Gamma \approx 0.5$ ions nm^{-2}, which exceeds that of Pt/WO_3 ($k_{vis} = (0.46 \pm 0.13)$ h^{-1}). Furthermore, the plot of k_{UV} against Γ exhibits a volcano-type curve with a maximum of (6.9 ± 0.8) h^{-1} at $\Gamma \approx 0.5$ ions nm^{-2}, which is greater than those for pristine P-25 and Pt/WO_3 by factors of 4.2 and 26, respectively. No iron ions were detected from the solutions after the reaction. As a gas-phase test reaction, the photocatalytic decomposition of CH_3CHO, a typical volatile organic compound, was carried out. Irradiation with visible light ($\lambda > 400$ nm, $I_{420-485\,nm} = 1.3$ mW cm^{-2}) or UV light ($330 < \lambda < 400$ nm, $I_{320-400\,nm} = 1.6$ mW cm^{-2}) to $(FeO_x)_m$/P-25 caused decomposition of CH_3CHO. Figure 3d shows the values of k_{vis} and k_{UV} as a function of Γ. Convex curves reaching maxima at $\Gamma \approx 0.1$ ions nm^{-2} are observed. $(FeO_x)_m$/P-25 shows a noticeable visible-light activity for the CH_3CHO decomposition, while the k_{UV} value is 6.4 times larger than that for P-25. Similar remarkable enhancement effects on the decompositions of 2-NAP (Supporting Information, Figure S3) and CH_3CHO (Supporting Information, Figure S4) are also obtained for ST-01. Clearly, this chemical surface modification causes the visible-light activity and a concomitant large increase in UV-light activity.

X-ray photoelectron spectroscopic (XPS) measurements were performed for gaining the information on the filled

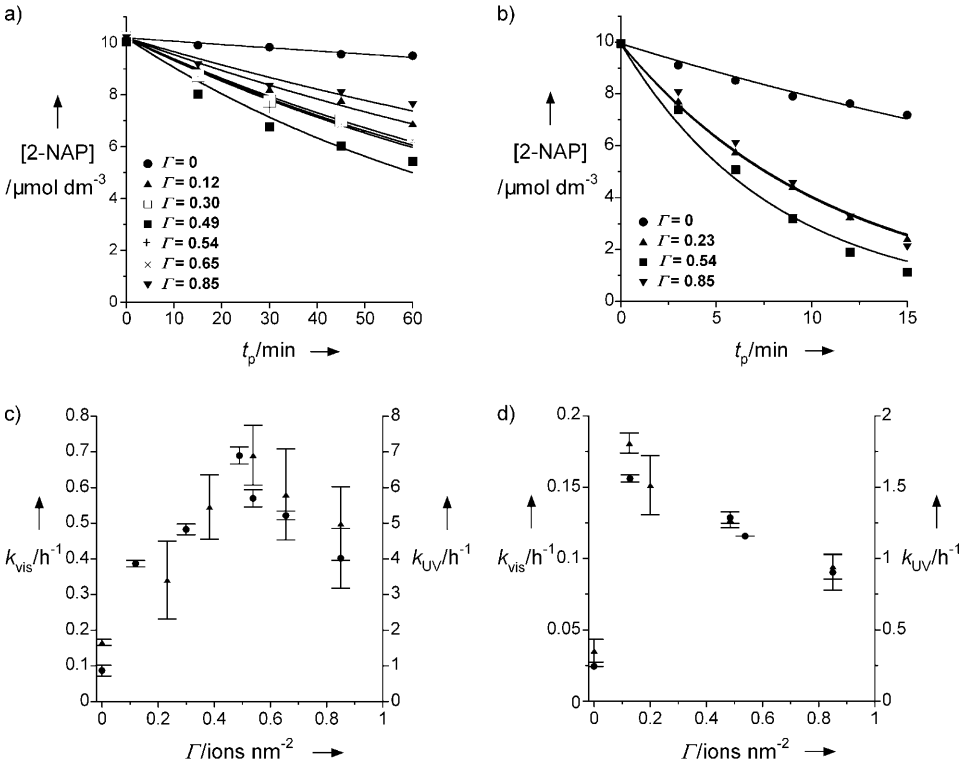

Figure 3. Photocatalytic activity of $(FeO_x)_m$/p-25. a) Time courses for 2-NAP decomposition under irradiation at $\lambda > 400$ nm. b) Time courses for 2-NAP decomposition under irradiation at $330 < \lambda < 400$ nm. c) Plots of the pseudo rate constants for 2-NAP decomposition under irradiation at $\lambda > 400$ nm (k_{vis}, ●) and at $330 < \lambda < 400$ nm (k_{UV}, ▲) vs. Γ. d) Plots of the pseudo rate constants for CH_3CHO decomposition under irradiation at $\lambda > 400$ nm (k_{vis}, ●) and at $330 < \lambda < 400$ nm (k_{UV}, ▲) vs. Γ.

energy levels of $(FeO_x)_m/TiO_2$. Figure 4a shows the valence-band (vb) XPS spectra for $(FeO_x)_m/TiO_2$. The emission from the O 2p vb extends from 3 to 9 eV. Closer inspection of the vb top (inset in Figure 4a) indicates its rise, ranging from 0.2 to 0.4 eV, with an increase in Γ, which is comparable with the decrease in E_g with the surface modification. The effective mixing between the surface Fe^{3+} levels and O 2p owing to the Ti_s–O–Fe interfacial bond is considered to yield a surface d sub-band, which disperses around the energy level to overlap with the vb(TiO_2). This interpretation explains the net decrease in the E_g of TiO_2. From the E_g for $(FeO_x)_m(\Gamma \approx 0.5)$/$TiO_2$ (ca. 2.9 eV), the top of the surface d sub-band is estimated to be situated at +2.4 V versus the standard hydrogen electrode (SHE).[22] The Fe 2p binding energy is sensitive to the oxidation state in the Fe compounds. Figure 4b shows Fe 2p XPS spectra for several iron oxides. The Fe $2p_{3/2}$ binding energies for α-Fe_2O_3 and FeO are (710.6 eV) and (709.2 eV), respectively. The value for $(FeO_x)_m/TiO_2$, which is (709.7 ± 0.5) eV, indicates that iron has a 2+/3+ mixed-valence state. XPS measurements confirmed the iron oxidation state of $(FeO_x)_n/TiO_2$-(rutile) to be 2+, which was ascribed to the reduction of Fe^{3+} ions under high-vacuum conditions.[15] However, if it is true, α-Fe_2O_3 should also undergo the reduction. Consequently, the electron transfer from TiO_2 to the as-formed $(FeO_x)_m$ is suggested to occur. The equilibrium potential of $(FeO_x)_m$/mp-TiO_2/FTO in the dark (E_{eq}) corresponds to its Fermi energy (E_F).[23] As a result of the increase in Γ, the E_{eq} increases; that is, E_F falls. Evidently, electron transfer from TiO_2 to $(FeO_x)_m$ results in a decrease in the E_F of $(FeO_x)_m$/mp-TiO_2/FTO (Supporting Information, Figure S5a). Importantly, the O_2 reduction potential of mp-TiO_2/FTO under UV-light irradiation shifts towards the positive direction by as much as 0.8 V with the iron surface modification (Supporting Information, Figure S5b). Thus, the $(FeO_x)_m$ species drastically promotes the electron transfer from TiO_2 to O_2.

On the basis of these results, we propose an energy-band diagram for $(FeO_x)_m/TiO_2$ (Scheme 1). The strong absorption of visible light triggers the electronic excitation from the surface d sub-band to the cb(TiO_2) (p_1). The holes generated in the surface d sub-band take part in the oxidation process without diffusion (p_2),[24] while the excited electrons efficiently reduce O_2 (p_3). Upon illumination by UV light (p_4), both hole transfer from the vb(TiO_2) to the surface d sub-band (p_5) and the surface d level-mediated electron transfer from the cb(TiO_2) to O_2 (p_3) enhance the charge separation to increase the photocatalytic activity. These concerted effects can lead to the visible-light activity and the remarkable increase in the UV-light activity. In the low Γ region, the photocatalytic activity increases with increasing Γ because of the increase in the light-absorption efficiency. Meanwhile, the excess Γ

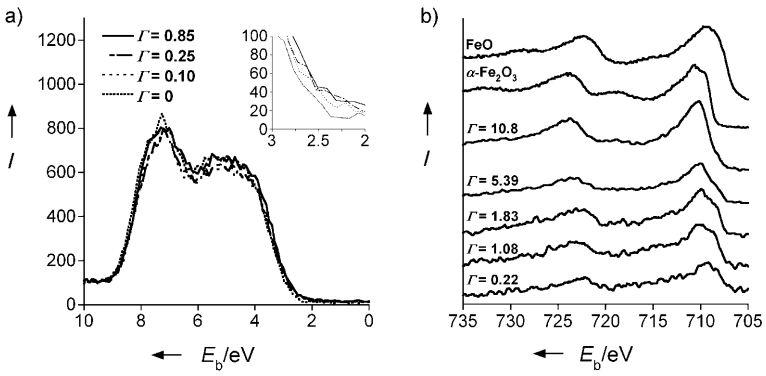

Figure 4. Electronic properties of $(FeO_x)_m/TiO_2$. a) Valence-band XPS spectra for $(FeO_x)_m$/P-25. b) Fe 2p XPS spectra for $(FeO_x)_m$/P-25, α-Fe_2O_3, and FeO.

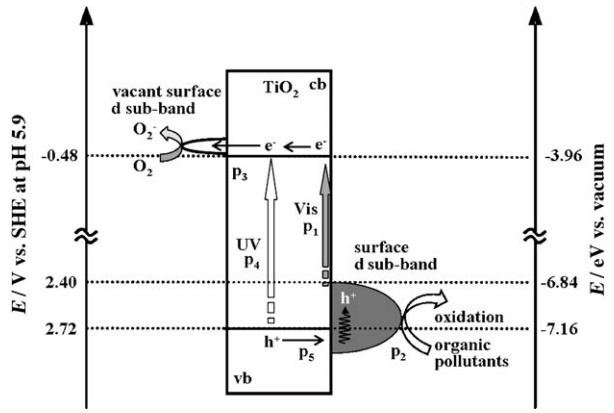

Scheme 1. Energy band diagram for $(FeO_x)_m/TiO_2$. The position of the vacant d levels is assumed to be close to that of iron doped into rutile TiO_2.[25]

would cause the drop of E_F to lower the reducing power of the excited electrons or the rise in the top of the surface d sub-band to reduce the hole oxidation power, and thus the photocatalytic activity falls. Consequently, an optimum Γ value is present. The fact that Fe^{3+} doping is effective only for quantum-sized TiO_2[10] can be explained within the framework; that is, in such a small TiO_2 aprticle, a part of the doped Fe^{3+} ions would form the surface oxide species. Scheme 1 also rationalizes a previous important finding in the $(FeO_x)_n/TiO_2$(rutile) system that the photoacoustic signal owing to Ti^{3+} formation intensifies by surface Fe^{3+} modification under visible-light irradiation in an N_2 atmosphere containing C_2H_5OH, whereas it declines under UV-light irradiation in air with C_2H_5OH.[14] The visible-light-induced electronic excitation accumulates electrons in TiO_2 to yield Ti^{3+} ions without O_2. Upon UV-light irradiation with O_2, the smooth consumption of the excited electrons by the surface d level-mediated O_2 reduction decreases the Ti^{3+} density.

In summary, the electronic modification of TiO_2 with the formation of extremely highly dispersed surface iron oxide species using the CCC technique has given rise to noticeable visible-light activity with a simultaneous large increase in activity under illumination with UV light. This simple and inexpensive technique can easily be applied to highly active TiO_2 particles and films hitherto developed to expand their applications to the environmental remediation and solar energy conversion.

Experimental Section

The TiO_2 samples that were used, which have the highest level of photocatalytic activities for commercial samples, were P-25 (anatase/rutile = 4:1 w/w), specific surface area $S = 50\ m^2 g^{-1}$, Degussa) and ST-01 (anatase, $S = 309\ m^2 g^{-1}$, Ishihara Sangyo). These TiO_2 particles with a mean size of 20 nm (PST-18NR, Nikki Syokubai Kasei) was coated on film-coated tin oxide (FTO) glass substrates ($12\ \Omega\ \square^{-1}$) by a squeegee method, and the sample was heated in air at 773 K to form mp-TiO_2 films.

After TiO_2 particles (1 g) or mesoporous TiO_2 nanocrystalline film-coated SnO_2 substrates (mp-TiO_2/FTO, 25 mm × 50 mm) had been added to of a [Fe(acac)$_3$] solution (solvent: 100 mL of ethanol/*n*-hexane = 3:17 v/v), they were allowed to stand for 24 h at 298 K. Unless otherwise noted, the [Fe(acac)$_3$] concentration was maintained at $6.5 \times 10^{-4}\ mol\,dm^{-3}$. The resulting samples were washed repeatedly with the same solvent to remove physisorbed complexes and then dried, followed by heating in air at 773 K for 1 h. These procedures were repeated to control the Fe loading amount.

UV/Vis diffuse reflectance spectra of FeO_x/TiO_2 and FeO_x/mp-TiO_2 were recorded on a Hitachi U-4000 spectrophotometer. The spectra were converted into the absorption spectra by using the Kubelka–Munk function. Fe K edge XAFS spectra were measured on the BL14B2 line at SPring-8. Spectra of $(FeO_x)_m/TiO_2$ and $(FeO_x)_n/TiO_2$ at the Fe K edge were recorded in fluorescence mode and those of reference samples in transmission mode. Data reduction was performed using the REX2000 program (Rigaku). XPS measurements were performed using a Kratos Axis Nova X-ray photoelectron spectrometer with a monochromated AlK_α X-ray source ($h\nu$ = 1486.6 eV) operated at 15 kV and 10 mA. The take-off angle was 90°, and multiplex spectra were obtained for Fe_{2p}, O_{1s}, and Ti_{2p} photopeaks. All of the binding energies (E_B) were referenced with respect to the C_{1s} at 284.6 eV.

The equilibrium potential and cyclic voltammograms of the $(FeO_x)_m$/mp-TiO_2/FTO electrodes were measured in a $0.1\ mol\,dm^{-3}$ Na_2SO_4 electrolyte solution in a regular three-electrode electrochemical cell using a galvanostat/potentiostat (HZ-5000, Hokuto Denko). Glassy carbon and an Ag/AgCl electrode (TOA-DKK) were used as a counter electrode and a reference electrode, respectively.

Photocatalytic activity evaluation: In both the decompositions of 2-naphthol (2-NAP) and CH_3CHO, the reaction cells were irradiated with a Xe lamp (Wacom XRD-501SW) through a band-pass filter (D33S, AGC Techno Glass) superposed on a piece of FTO-coated glass that transmits only the 330–400 nm range for the UV-light photocatalytic activity evaluation and a high-pass filter (L-42, Toshiba) to cut off UV light for the visible-light-induced activity test. TiO_2 or $(FeO_x)_m/TiO_2$ particles (0.1 g) were placed in a solution of 2-NAP ($1.0 \times 10^{-5}\ mol\,dm^{-3}$, solvent: 50 mL of acetonitrile/water = 1:9999 v/v) in a borosilicate glass container and irradiated. A sample of the solution (2 mL) was taken every 15 min and the electronic absorption spectra of the reaction solutions were measured using a spectrometer (Shimadzu, UV-1800) to determine 2-NAP concentration from the absorption peak at 224 nm. A 594 ppm standard CH_3CHO gas (CH_3CHO/N2) was introduced into a reaction chamber (0.64 L) and diluted with air such that its initial concentration was kept within the 400 ppm range. After the adsorption equilibrium of CH_3CHO on TiO_2 or $(FeO_x)_m/TiO_2$ particles (0.15 g) had been achieved under dark conditions, irradiation was carried out at room temperature. The concentration of CH_3CHO was determined as a function of time by gas chromatography (Shimadzu, GC-9A) with a Shincarbon A f.i.d. column (3 mmϕ × 3 m): injection and column temperatures were 343 K, and N_2 was used as a carrier gas.

Received: December 14, 2010
Published online: March 11, 2011

Keywords: electron transfer · iron oxide · photocatalysis · surface modification · TiO_2

[1] T. Kawahara, Y. Konishi, H. Tada, N. Tohge, J. Nishii, S. Ito, *Angew. Chem.* **2002**, *114*, 2935; *Angew. Chem. Int. Ed.* **2002**, *41*, 2811.
[2] R. Asahi, T. Morikawa, T. Ohwaki, K. Aoki, Y. Taga, *Science* **2001**, *293*, 269.
[3] S. U. M. Khan, M. Al-Shahry, W. B. Ingler, Jr., *Science* **2002**, *297*, 2243.
[4] N. Serpone, *J. Phys. Chem. B* **2006**, *110*, 24287.
[5] H. Zhang, G. Chen, D. W. Bahnemann, *J. Mater. Chem.* **2009**, *19*, 5089.

[6] M. Anpo, M. Takeuchi, *J. Catal.* **2003**, *216*, 505.
[7] M. Kitano, K. Funatsu, M. Matsuoka, M. Ueshima, M. Anpo, *J. Phys. Chem. B* **2006**, *110*, 25266.
[8] G. Liu, L. Wang, H. G. Yang, H.-M. Cheng, G. Q. Lu, *J. Mater. Chem.* **2010**, *20*, 831.
[9] M. I. Litter, J. A. Navio, *J. Photochem. Photobiol. A* **1996**, *98*, 171.
[10] W. Choi, A. Termin, M. R. Hoffmann, *Angew. Chem.* **1994**, *106*, 1148; *Angew. Chem. Int. Ed. Engl.* **1994**, *33*, 1091.
[11] K. Nagaveni, M. S. Hedge, G. Madras, *J. Phys. Chem. B* **2004**, *108*, 20204.
[12] N. Serpone, D. Lawless, J. Disdier, J.-M. Hermann, *Langmuir* **1994**, *10*, 643.
[13] H. Kisch, L. Zhang, C. Lange, W. F. Maier, C. antonius, D. Meissner, *Angew. Chem.* **1998**, *110*, 3201; *Angew. Chem. Int. Ed.* **1998**, *37*, 3034.
[14] N. Murakami, T. Chiyoya, T. Tsubota, T. Ohno, *Appl. Catal. A* **2008**, *348*, 148.
[15] H. Yu, H. Irie, Y. Shimodaira, Y. Hosogi, Y. Kuroda, M. Miyauchi, K. Hashimoto, *J. Phys. Chem. C* **2010**, *114*, 16481.
[16] H. Tada, *Encyclopedia of Surface and Colloid Science* (Ed.: A. T. Hubbard), Marcel Dekker, New York, **2002**.
[17] J. A. Navio, G. Colon, M. I. Litter, G. N. Bianco, *J. Mol. Catal. A* **1996**, *106*, 267.
[18] C.-Y. Wang, D. W. Bahnemann, J. K. Dohrmann, *Chem. Commun.* **2000**, 1539.
[19] R. Abe, H. Takami, N. Murakami, B. Ohtani, *J. Am. Chem. Soc.* **2008**, *130*, 7780.
[20] T. E. Westre, P. Kennepohl, J. G. DeWitt, B. Hedman, K. O. Hodgson, E. I. Solomon, *J. Am. Chem. Soc.* **1997**, *119*, 6297.
[21] K.-i. Yamada, N. Mukaihata, T. Kawahara, H. Tada, *Langmuir* **2007**, *23*, 8593.
[22] M. Grätzel, F. P. Rotzinger, *Chem. Phys. Lett.* **1985**, *118*, 474.
[23] T. Kiyonaga, Q. Jin, H. Kobayashi, H. Tada, *ChemPhysChem* **2009**, *10*, 2935.
[24] H. Irie, T. Shibanuma, K. Kamiya, S. Miura, T. Yokoyama, K. Hashimoto, *Appl. Catal. B* **2010**, *96*, 142.
[25] K. Mizushima, M. Tanaka, A. Asai, S. Iida, J. B. Goodenough, *J. Phys. Chem. Solids* **1979**, *40*, 1129.

